JOURNAL OF GEOPHYSICAL RESEARCH, VOL. 102, NO. B6, PAGES 12,123–12,138, JUNE 10, 1997

Listric normal faulting on the Cascadia continental margin

Lisa C. McNeill[1], Kenneth A. Piper[2], Chris Goldfinger[3],
LaVerne D. Kulm[3], and Robert S. Yeats[1]

Abstract. Analysis of multichannel seismic reflection profiles reveals that listric normal faulting is widespread on the northern Oregon and Washington continental shelf and upper slope, suggesting E-W extension in this region. Fault activity began in the late Miocene and, in some cases, has continued into the Holocene. Most listric faults sole out into a subhorizontal décollement coincident with the upper contact of an Eocene to middle Miocene mélange and broken formation (MBF), known as the Hoh rock assemblage onshore, whereas other faults penetrate and offset the top of the MBF. The areal distribution of extensional faulting on the shelf and upper slope is similar to the subsurface distribution of the MBF. Evidence onshore and on the continental shelf suggests that the MBF is overpressured and mobile. For listric faults which become subhorizontal at depth, these elevated pore pressures may be sufficient to reduce effective stress and to allow downslope movement of the overlying stratigraphic section along a low-angle (0.1°-2.5°) detachment coincident with the upper MBF contact. Mobilization, extension, and unconstrained westward movement of the MBF may also contribute to brittle extension of the overlying sediments. No Pliocene or Quaternary extensional faults have been identified off the central Oregon or northernmost Washington coast, where the shelf is underlain by the rigid basaltic basement of the Siletzia terrane. Quaternary extension of the shelf and upper slope is contemporaneous with active accretion and thrust faulting on the lower slope, suggesting that the shelf and upper slope are decoupled from subduction-related compression.

Introduction and Previous Work

Listric normal faulting is a common feature of passive margins, where fault movement contributes to crustal thinning and margin subsidence. Extension and normal faulting are also a fairly common phenomenon on convergent margins throughout the world. Examples include the forearcs of southern Peru-northern Chile [*Li*, 1995], northern Peru [*von Huene et al.*, 1989], the Middle America Trench off Costa Rica [*McIntosh et al.*, 1993] and Guatemala [*Aubouin et al.*, 1982], and the Japan Trench [*Karig et al.*, 1983; *von Huene and Lallemand*, 1990]. Extension is often associated with basal or frontal subduction erosion or nonaccretion [*von Huene and Scholl*, 1991; *McIntosh et al.*, 1993]. Decoupling by high pore pressures and reduced basal shear stress may also lead to extension in a convergent tectonic setting [*Dahlen*, 1984; *von Huene et al.*, 1989].

The Cascadia subduction zone (Figure 1) is characterized by active accretion with ample evidence of late Quaternary convergence and compressional folding on the continental slope (Figure 2a) [*Silver*, 1972; *Kulm et al.*, 1973; *Carson et al.*, 1974; *Goldfinger et al.*, 1992; *MacKay et al.*, 1992]. Older (late Pliocene to early Quaternary) compressional structures have been mapped by previous workers [*Silver*, 1972; *Kulm and Fowler*, 1974; *Wagner et al.*, 1986; *Snavely*, 1987; *Goldfinger et al.*, 1992] on the continental shelves of Oregon and Washington (Figure 2a). This study enlarges on the work of *Cranswick and Piper* [1992] which revealed the existence of active crustal extensional structures on the Washington and northern Oregon shelf and upper slope. The extent, morphology, and possible causes of these extensional features have been further documented by *Piper* [1994], *Piper et al.* [1995], and *McNeill et al.* [1995]. Discovery of these extensional structures requires a reevaluation of structures previously interpreted as folds and faults related to plate convergence. This paper will focus on the morphology, structure, stratigraphy, and inferred mechanisms of normal faulting on the Cascadia margin.

Tectonic Setting

The Cascadia subduction zone is formed by the subduction of the oceanic Juan de Fuca and Gorda plates beneath the North American plate off the coast of northern California, Oregon, Washington, and Vancouver Island, British Columbia (Figure 1). The convergence rate is 42 mm/yr. directed N69°E at the latitude of Seattle according to the NUVEL-1 plate motion model (Figure 1) [*DeMets et al.*, 1990]. Juan de Fuca-North American convergence is oblique, with obliquity decreasing at 5 Ma due to clockwise rotation of the convergence vector [*Wilson*, 1993], and with distance along the margin from south to north, due to increasing distance from the pole of rotation and change in orientation of the margin. The submarine forearc widens from 60 km off southern Oregon to 150 km off the northern Olympic Peninsula of Washington, suggesting higher regional sedimentation rates to the north. Higher Pleistocene sedimentation rates in this region are also indicated by the Astoria and Nitinat Fans on the northern

[1] Department of Geosciences, Oregon State University, Corvallis.
[2] Minerals Management Service, Camarillo, California.
[3] College of Oceanic and Atmospheric Sciences, Oregon State University, Corvallis.

Paper number 97JB00728.
0148-0227/97/97JB-00728$09.00

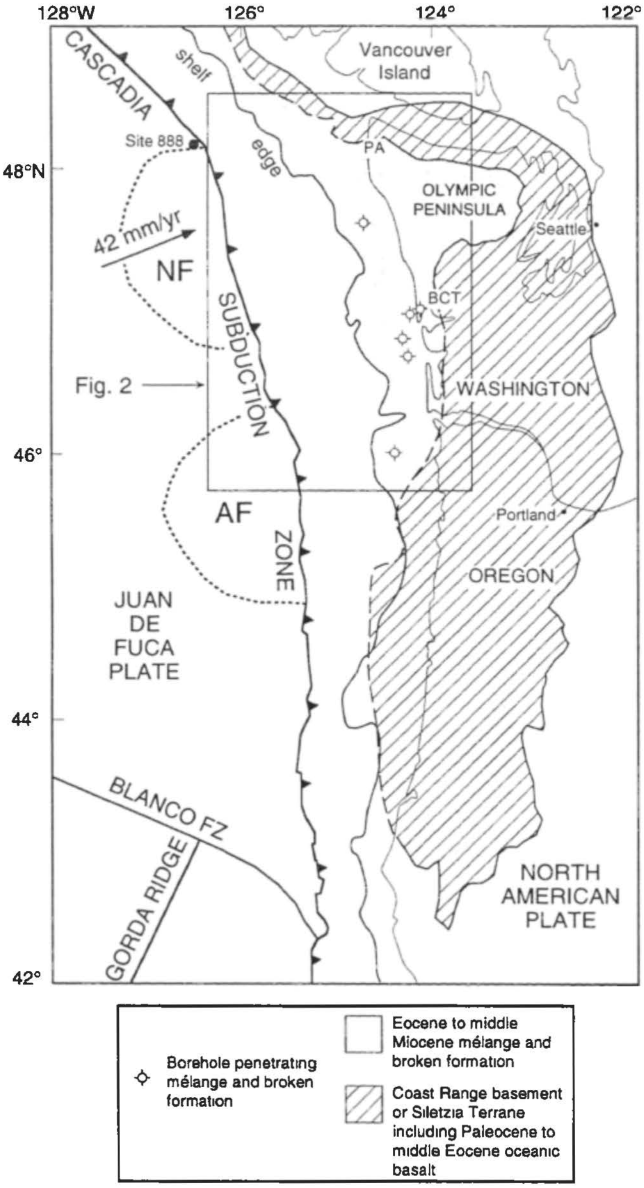

Figure 1. Map of the Cascadia subduction zone showing the study area (boxed) and underlying lithologies of the Oregon and Washington continental shelves (modified from *Snavely* [1987] and *Palmer and Lingley* [1989]). The northern Oregon and Washington shelf are underlain by mélange and broken formation (MBF) of the accretionary complex (Hoh rock assemblage of *Rau* [1973]) which extends landward onto the Olympic Peninsula, whereas the central Oregon shelf is underlain by oceanic basalt of the Siletz River Volcanics. Industry boreholes penetrating the MBF are also shown. PA, Point of the Arches, BCT, Big Creek Thrust. Submarine fans: NF, Nitinat Fan; AF, Astoria Fan. Position of Ocean Drilling Program Site 888 is shown. Plate convergence vector from *De Mets et al.* [1990].

Oregon and Washington abyssal plain (Figure 1). The accretionary complex comes onshore in Washington, where it is uplifted and eroded to form the core rocks of the Olympic Mountains. Much of onshore western Oregon and Washington and the continental shelf of Oregon are underlain by a basement of Paleocene to middle Eocene oceanic basalt with interbedded sediments, which is known as the Coast Range basaltic basement or Siletzia terrane (Figure 1). Currently active accretionary thrust faults on the lower slope are characterized by seaward vergent thrusts on the Oregon margin from 42° to 44°55'N and north of 48°08'N off Vancouver Island, British Columbia, and by landward vergent thrusts between 44°55' and 48°08'N, on the northern Oregon and Washington margins.

It has been suggested that growth faulting in association with mud diapiric intrusions or piercement structures are a common phenomenon on the Washington continental shelf [*Snavely*, 1987; *Snavely and Wells*, 1991]. *Snavely and Wells* [1991] note that several seismic profiles reveal west dipping listric normal faults at the shelf edge. They attribute fault movement to downslope movement following sediment loading and collapse of the shelf margin. Analysis of an extensive data set of proprietary migrated multichannel seismic reflection profiles (Figure 2b) reveals that these listric normal faults and nonlistric normal faults are fairly widespread on the mid to outer continental shelf and uppermost slope of the Washington and northernmost Oregon margins (Figure 2c) [*Piper*, 1994; *Piper et al.*, 1995; *McNeill et al.*, 1995]. The most prominent of these faults are listric normal faults which deform as much as 3 km of the uppermost sedimentary section. Other extensional structures are not listric in the reflection data, have minimal offset, and lack prominent growth strata. These faults may or may not be listric at depth below the interpretable part of the data. These faults will be examined and discussed collectively with the more clearly listric faults.

Stratigraphy and Uplift History

The continental shelf of Washington and the outer to midshelf of northernmost Oregon are underlain by a thick section of Eocene to middle Miocene mélange and broken formation (Figures 1 and 3) [*Snavely*, 1987]. The mélange and broken formation may also be present elsewhere on the Cascadia margin but not immediately underlying late Tertiary strata. The mélange and broken formation (MBF), known as the Hoh rock assemblage on the western Olympic Peninsula [*Rau*, 1973, 1975, 1979; *Orange et al.*, 1993], forms the uplifted accretionary complex of the Olympic Mountains (Figure 1) [*Tabor and Cady*, 1978]. *Snavely and Kvenvolden* [1989] have subdivided the coastal rocks into the middle to late Eocene Ozette mélange and the late Oligocene to middle Miocene Hoh rock assemblage, but *Orange et al.* [1993] were unable to distinguish between these two units. The Eocene to middle Miocene mélange and broken formation is not subdivided in this paper, according to the nomenclature of *Rau* [1973, 1975, 1979] and *Orange et al.* [1993] and is referred to as the MBF. The Hoh rock assemblage crops out along the coast approximately between Point of the Arches in the north and the Big Creek thrust in the south (Figure 1) [*Palmer and Lingley*, 1989]. Coastal outcrops of the Hoh rock assemblage contain both locally coherently stratified sandstones and siltstones, including turbidites, and chaotic assemblages of siltstone, sandstone, conglomerate, and altered volcanic blocks with a fine grained matrix of clay and siltstone ("tectonic mélange" of *Rau* [1973]). The weakness of the tectonic mélange is exemplified by slumping of coastal deposits and by the expansive nature of materials encountered by coastal and offshore industry boreholes [*Rau*, 1973]. To the west, beneath the Washington continental shelf, all industry boreholes reached the MBF (Figure 1) [*Snavely*,

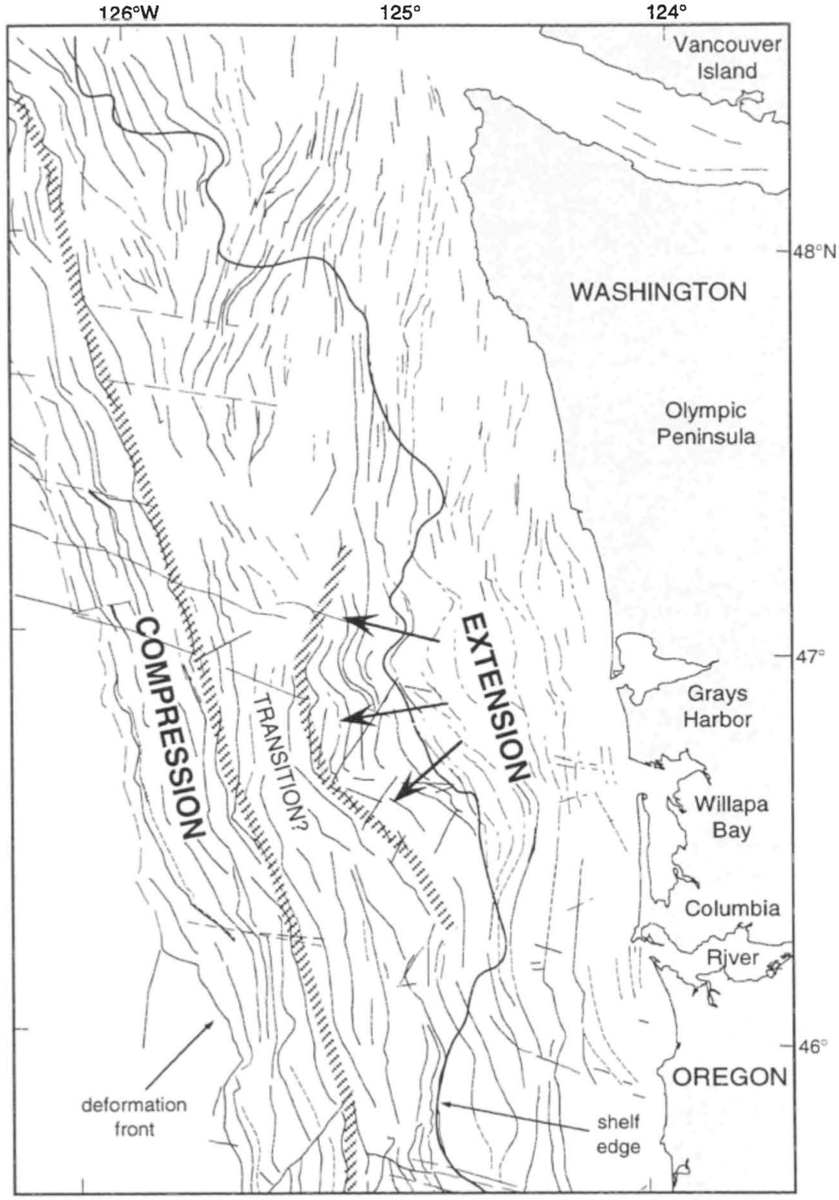

Figure 2a. Neotectonic map of the Washington and northern Oregon margins (modified from *McCaffrey and Goldfinger* [1995]) showing Quaternary (solid lines) and Pliocene and early Pleistocene (dashed lines) anticlinal fold axes and faults (synclinal fold axes removed for clarity). Dashed lines also indicate inferred structures. The map was compiled from interpretations of the following data sets: industry, government, and academic seismic reflection profiles (Figure 2b); bathymetry; side-scan sonar imagery; and submersible observations. Active compression in response to northeasterly convergence occurs on the lower slope (labeled "compression"). The shelf and upper slope are characterized by E-W extensional structures discussed in this paper (labeled "extension"), with evidence of N-S compression on the inner shelf. A zone exists where the extent of compression versus extension is presently uncertain (labeled "transition?"). Note that fold trends on the midslope wrap around a "protrusion" visible in bathymetry and the shelf edge opposite Grays Harbor, which is interpreted as the western edge of the MBF. Arrows indicate downslope movement of the MBF. North and south of the protrusion, the seaward extent of the MBF is unclear.

1987; *Palmer and Lingley*, 1989]. None of the boreholes reached units older than the Eocene MBF, but ~2 km of Eocene to middle Miocene sediments were encountered, which serves as a minimum thickness for the MBF on the midshelf. The precise extent of the MBF to the west is unclear, but its acoustic character in seismic reflection profiles, outlined below, suggests that the formation extends westward at least as far as the present shelf edge. *Snavely* [1987] inferred that the MBF extends to the midslope. The Astoria Formation and Nye Mudstone are the time and lithologic correlatives of portions of the Oligocene and Miocene Hoh rock assemblage on the northern Oregon shelf [*Palmer and Lingley*, 1989].

Rapid regional uplift of the present continental margin occurred toward the end of the middle Miocene, uplifting and eroding the MBF. Latest middle Miocene and late Miocene strata of the Montesano Formation deposited in middle

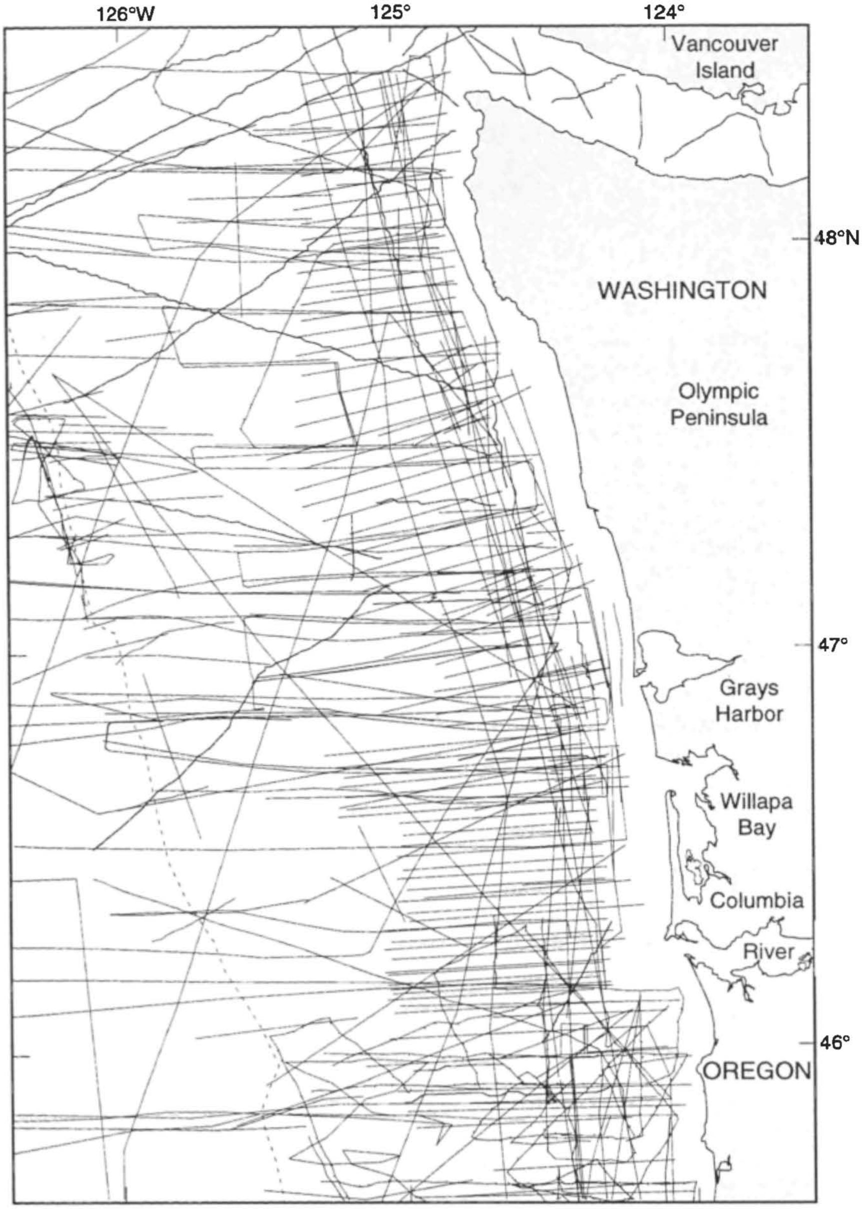

Figure 2b. Map of undifferentiated seismic reflection track lines from industry (public and proprietary), academic, and government sources. Profiles include single and multichannel and migrated and unmigrated data. Dashed line indicates the deformation front.

bathyal to neritic water depths (Figure 3) overlie the erosional angular unconformity and the MBF [*Palmer and Lingley*, 1989]. The Montesano Formation can be subdivided into three main units according to *Bergen and Bird* [1972]: lower claystone member; middle sandstone member; and upper siltstone member. Shallow water depths indicated by the sandstone member suggest that the present continental shelf developed in the late Miocene, at ~ 7Ma [*Palmer and Lingley*, 1989]. Development of the shelf is thought to be primarily a result of regional uplift and not simply shoaling through rapid deposition [*Bergen and Bird*, 1972]. Offshore paleobathymetry suggests primarily bathyal depths for the Montesano (S.D. Drewry et al., Minerals Management Service (MMS), unpublished work, 1993). Quinault- (and Quillayute-) equivalent Pliocene strata unconformably overlie the Montesano, as defined by *Palmer and Lingley* [1989], with onshore paleobathymetry indicating variable depositional depths, including bathyal, neritic, and neritic/littoral sequences (Figure 3) [*Rau*, 1970]. Offshore microfossil paleobathymetry records both bathyal and neritic depths (aforementioned MMS unpublished work). These Pliocene strata are, in turn, overlain by Pliocene and Pleistocene gravels [*Palmer and Lingley*, 1989]. Paleobathymetry [*Rau*, 1970; *Bergen and Bird*, 1972] suggests a net progressive shallowing through the Miocene and Pliocene, from bathyal to neritic, but episodic basinal downwarping within this period is indicated by the thick section of post-MBF sediments, as much as 2 km in places [*Snavely*, 1987], and variable paleowater depths within individual units (Figure 3).

Diapiric intrusions on the Washington continental shelf are largely rooted in the mélange and broken formation [*Snavely and Wagner*, 1982; *Snavely and Wells*, 1991]. Late Miocene

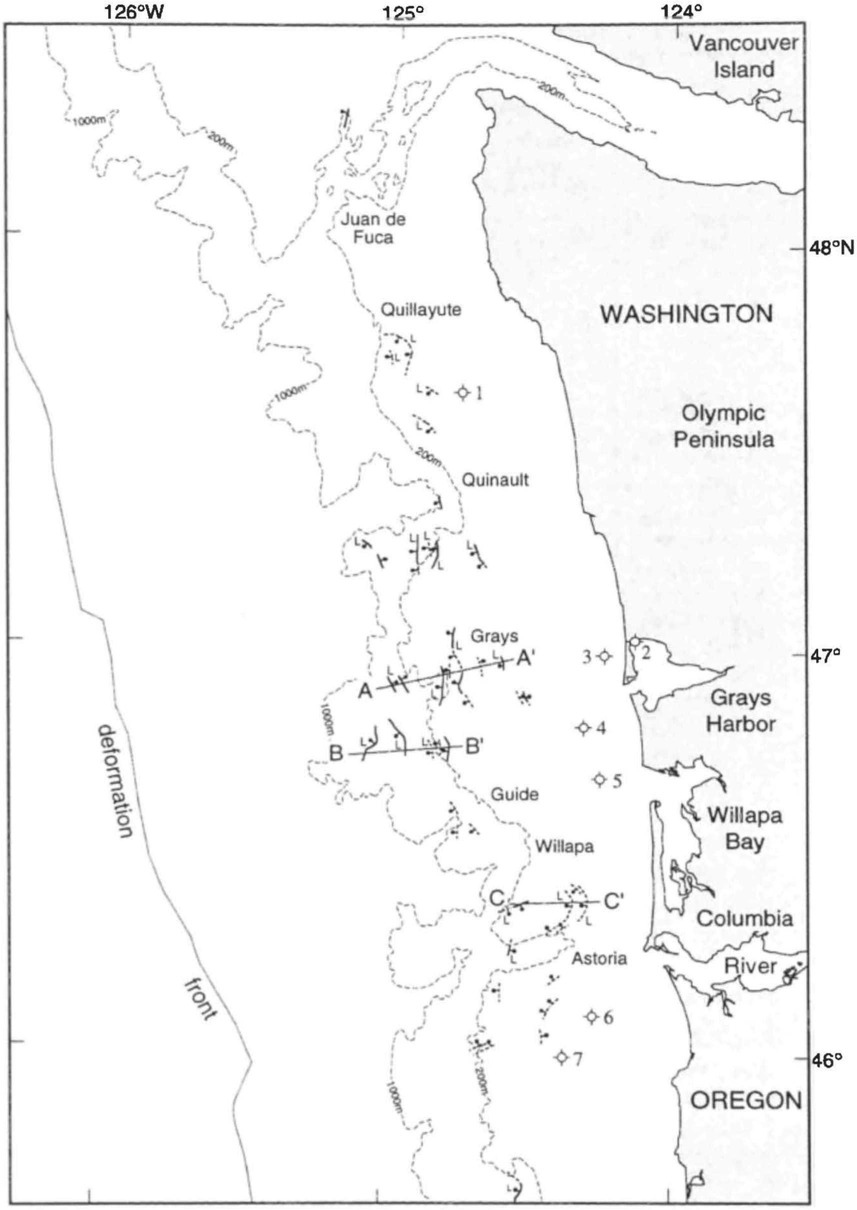

Figure 2c. Map of the study area locating major normal faults mapped in this study. Listric normal faults indicated by "L". The 200 m (approximating the shelf edge) and 1000 m bathymetric contours represented as dashed lines. Normal faults active in the latest Pleistocene and Holocene (deforming youngest sediments and/or seafloor) shown as solid lines; normal faults active in the Pliocene and early Pleistocene shown as dashed lines. Bar and ball indicate downthrown side of fault. Submarine canyons are labeled (Juan de Fuca to Astoria) and A-A', B-B', and C-C' represent seismic reflection profiles shown in Figures 5, 6, and 7, respectively. Industry boreholes on the continental shelf and in Grays Harbor area (open circles): 1, Pan American P-0141; 2, Sunshine Medina; 3, Union Tidelands; 4, Shell P-0155; 5, Shell and Pan American P-0150; 6, Shell P-075; 7, Shell P-072. Grays Canyon area (Figure 4) shown as box.

and younger sediments thin and onlap against these diapirs, suggesting that growth began in the late Miocene [*Snavely*, 1987].

Seismic Reflection Data Acquisition and Processing

Multichannel seismic reflection data used in this study were collected during three acquisition phases. Phase 1 data were acquired using a four-gun aquapulse array and 110 foot shot point interval, yielding 46-fold data. Phase 2 data were acquired using a 16-gun air gun array and 328 foot shot point interval, yielding 48-fold data. Processing for phases 1 and 2 included minimum phase inverse filter deconvolution and finite difference poststack migration, with approximate frequency filters of 10-55 Hz in the upper section and 5-25 Hz in the lower section. Phase 3 data were acquired using a 24-gun air gun array and 87.4 foot shot point interval, yielding 60-fold data. Processing included minimum phase inverse filter deconvolution and high-dip residual poststack migration, with

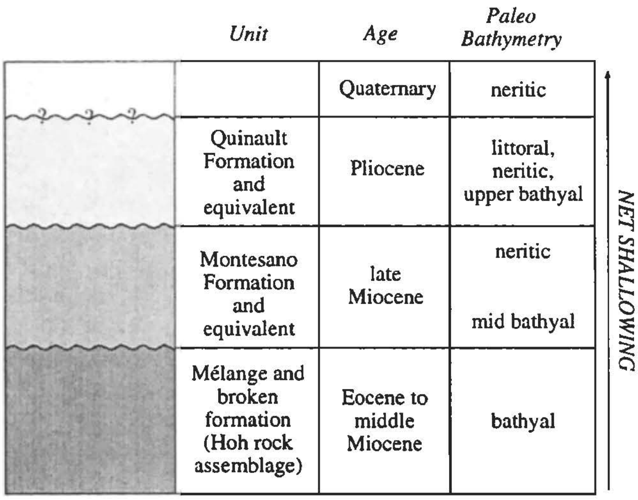

Figure 3. Stratigraphy of the Washington continental shelf as inferred from outcrops on the western Olympic Peninsula and lithologies penetrated by industry boreholes on the continental shelf [*Palmer and Lingley*, 1989]. Paleobathymetry determined from biostratigraphic analysis of onshore and offshore wells and onshore outcrops using benthic foraminifera [*Rau*, 1970; *Bergen and Bird*, 1972] (summarized by *Palmer and Lingley* [1989]). The Miocene through Quaternary sequence indicates net shallowing. Shading patterns correspond to units in seismic profile interpretations of Figures 5-7.

approximate frequency filters of 8-55 Hz in the upper section and 5-25 Hz in the lower section. The seismic reflection data are shown here as migrated time sections.

Delineation of Seismic Stratigraphic Units

Delineation of stratigraphic units (Figure 3) shown in seismic line interpretations, A-A', B-B', and C-C' (Figures 2c and 4 for location; Figures 5, 6, and 7), has been determined from interpretations of the following industry boreholes on the continental shelf: Pan American P-0141; Shell P-0155; Shell/Pan American P-0150; and Shell P-075 and P-072 (locations shown in Figure 2c). Depths to unit surfaces were determined using available interpretations of industry borehole logs and cuttings [*Palmer and Lingley*, 1989; S.D. Drewry et al., MMS unpublished work, 1993]. Benthic foraminifera biostratigraphy of the Pacific Northwest [*Rau*, 1981; *Bergen and Bird*, 1972] is based on correlations with Californian benthic foraminifera stages of *Kleinpell* [1938], *Natland* [1952], and *Mallory* [1959]. To locate approximate lithostratigraphic boundaries in the seismic records, these depths were converted to travel time using seismic refraction survey velocities of the Washington margin [*Shor et al.*, 1968; *McClain*, 1981] and sonic logs where available. Unit tops were then correlated along the network of seismic profiles. The distance of the correlation from its source was often large, and reflectors were often difficult to trace, thus introducing some degree of uncertainty into the stratigraphic interpretations shown in Figures 5, 6, and 7. However, the Eocene to middle Miocene MBF, reached by all Washington shelf industry boreholes (Figure 1), has a distinct acoustic character, allowing easy identification and traceability; the discontinuous and intensely sheared nature of the MBF results in similarly discontinuous seismic reflectors. This unit can be recognized below ~2 s two-way travel time (TWTT) in Figure 5, in contrast with the well-stratified overlying units. While correlation errors were compounded by minor differences between biostratigraphic calls reported in the literature, these correlation methods were considered sufficient and appropriate for this study. There is no evidence of the base of the MBF unit in available seismic reflection profiles or refraction velocity profiles. Thus this method cannot be used to determine the thickness of this unit.

Distribution and Morphology of Normal Faults

Well-defined normal faults occur on the middle to outer continental shelf and upper slope of the northern Oregon and Washington margins (Figure 2c). The most spectacular of these faults in seismic reflection profiles are listric growth faults shallowing to subhorizontal dips at depth ("L" in Figure 2c). In general, listric normal faults showing activity in the Pliocene (and possibly early Pleistocene) tend to be located on the midshelf and outer shelf (dashed lines); more recently active Holocene and late Pleistocene faults (solid lines), deforming uppermost sediments and/or the seafloor, occur throughout the midshelf to outer shelf and on the uppermost slope but more commonly near the shelf break. For all major normal faults (listric and apparently nonlistric), a tentative correlation can be made between age and location, with the more recently active structures located closer to the shelf break. All major extensional faults are located in < 1000 m water depth (Figure 2c). The distribution of normal faults in apparent E-W bands, as shown in Figure 2c, is not an artifact of the grid of seismic data.

Where their orientation can be determined, most normal faults identified in this study strike approximately north-south or parallel to the main trend of the shelf edge (Figure 2c). Those faults which can be traced across several seismic profiles often have a concave-seaward arcuate fault trace (e.g., line C-C', Figure 2c). More than 80% of the major normal faults mapped dip seaward. The apparent short fault length, usually < 5 km and no longer than 20 km, is not a function of the spacing of seismic reflection profiles.

A neotectonic map of the Grays Canyon region is shown in Figure 4, part of a map of the Oregon and Washington margin (Figure 2a) [*Goldfinger et al.*, 1992; *McCaffrey and Goldfinger*, 1995; C. Goldfinger and L.C. McNeill, manuscript in preparation, 1997]. Faults and folds are separated into those active during the Pliocene and earliest Pleistocene (dashed) and those active during the late Pleistocene and Holocene ("active", solid). Figure 4 also gives the locations of two seismic profiles, A-A' and B-B' (Figures 5 and 6), which cross several prominent normal faults ("N" and "LN").

The listric normal faults are characterized by regular growth strata which indicates continuous rather than sporadic activity beginning in the late Miocene (Figures 5, 6, and 7). Growth faulting may be partially responsible for the thick sections of post-middle Miocene strata observed in continental shelf basins. Half-graben basins associated with these listric faults are relatively narrow [*Snavely and McClellan*, 1987; *Snavely and Wells*, 1991], between 4 and 10 km (perpendicular to the fault), with basinal sediment thicknesses up to 2-3 km. Normal faults deform and offset sediments of late Miocene, Pliocene, and, in some cases, Quaternary age. Rollover folds

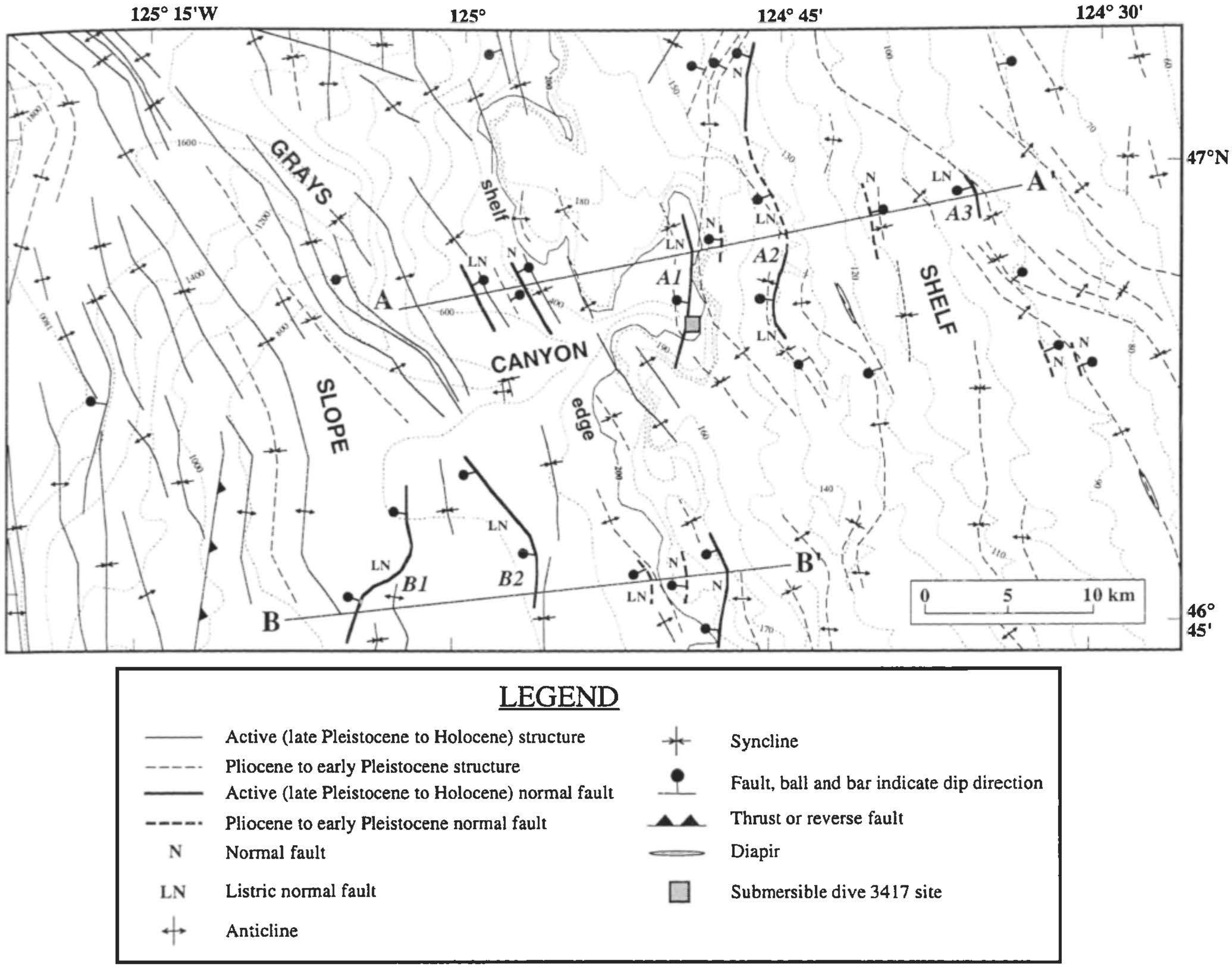

Figure 4. Neotectonic and bathymetric map of the Grays Canyon outer shelf and upper slope region. See Figure 2a for sources of interpretation. See Figure 2c for location of line A-A' and B-B'. Line A-A' crosses three major seaward dipping listric normal faults, A1, A2, and A3 (see Figure 5). Fault A1 at the head of Grays Canyon was a target for side-scan sonar surveys and submersible dives during 1994. The position of dive 3417 is indicated by the shaded box. Line B-B' crosses listric normal faults, B1 and B2 (see Figure 6). Other normal faults are indicated by "N" (nonlistric normal faults) and "LN" (listric normal faults). Bathymetric contours are spaced every 200 m on the slope and every 10 m on the shelf. The 200 m contour broadly defines the shelf break. Owing to scale constraints, not all structures shown in seismic line interpretations (Figures 5 and 6) are shown.

are common in hanging wall growth strata of listric faults with major offset (A1, Figure 5), similar to growth faults on passive margins [*Busch*, 1975]. In some cases, fault splays occur in the uppermost sedimentary section, producing a wedge of faulted material (B2, Figure 6). For the majority of listric faults, the fault dip shallows to a subhorizontal décollement, approximately coincident with the upper contact of the MBF (Figures 5 and 7). This décollement occurs at travel times of up to 2.5-3.0 s TWTT, equivalent to ~ 3.0 km depth (Figure 5). This corresponds to about 25-30% of the total forearc sedimentary section above the subducting basaltic slab at the continental shelf edge, which is estimated to be at a depth of 10-12 km [*Brandon and Calderwood*, 1990]. For other listric faults (e.g., eastern end of Figure 6), the fault plane is more steeply dipping and apparently penetrates the top of the MBF. The fault plane may become subhorizontal within the MBF unit but is not imaged in the seismic section; faults therefore offset and deform undetermined thicknesses of the MBF unit. In both cases, extension is not a superficial effect.

Many of the normal faults cut the seafloor, indicating Holocene activity, and several produce measurable fault offsets in seismic sections (Figure 6). Faults B1 and B2 produce a seafloor offset of ~ 25 m (Figure 6). Fault A1, which is located at the head of Grays Canyon (Figures 4 and 5), also shows significant seafloor offset, although the scarp is accentuated by erosion and slumping at the head of the submarine canyon. This listric normal fault was the target of sidescan sonar and submersible investigations during an Oregon State University scientific cruise sponsored by the NOAA National Undersea

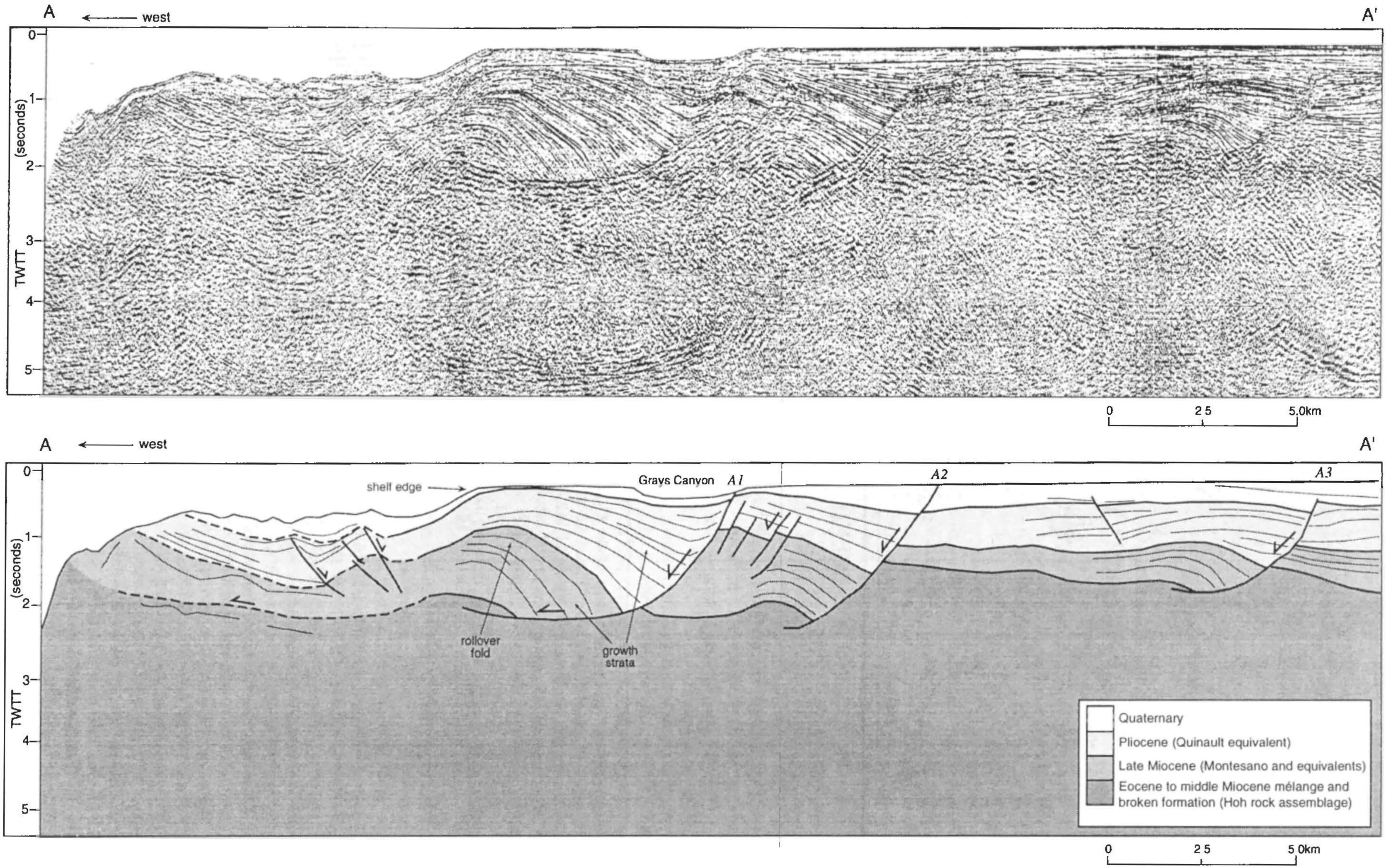

Figure 5. (Top) E-W migrated multichannel seismic reflection profile A-A' on the central Washington continental shelf and upper slope with (bottom) interpretive line drawing. See Figures 2c and 4 for location. Three major listric faults, A1, A2 and A3, are crossed by the profile including fault A1 at the head of Grays Canyon, a target of submersible dives in 1994. Listric faults deform late Miocene to Quaternary sediments with minor deformation of the uppermost mélange and broken formation. Faults A1 and A2 show evidence of recent activity including deformed Holocene sediments, seafloor offset, and methane-derived carbonates resulting from fluid venting. The listric faults sole out at depth into a décollement close to or at the upper contact of the mélange and broken formation. The faults are characterized by growth strata and rollover folds. TWTT, two-way travel time. Vertical exaggeration ~ 2:1 at seafloor.

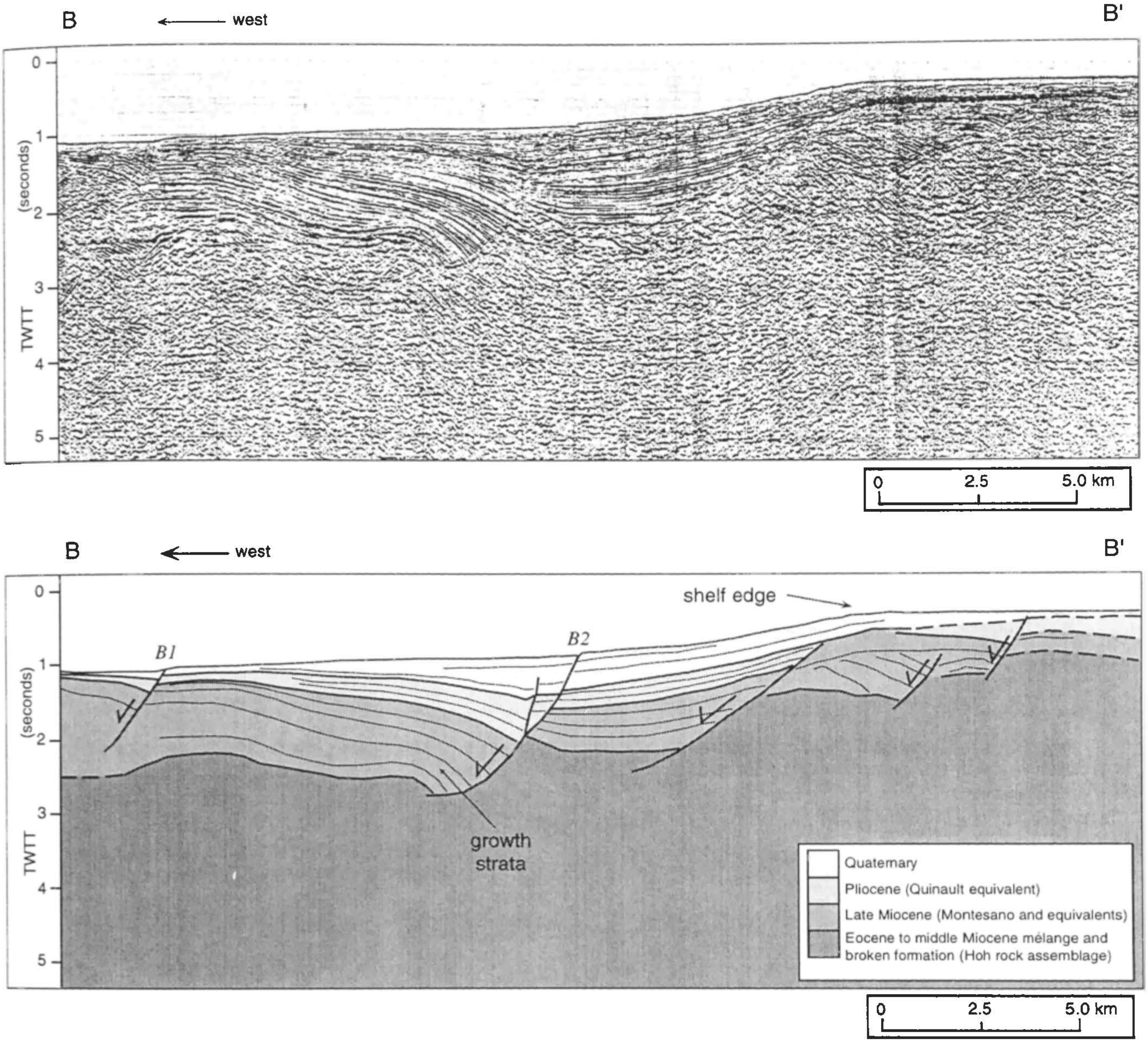

Figure 6. (Top) E-W migrated multichannel seismic reflection profile B-B' on the central Washington upper slope and shelf edge with (bottom) interpretive line drawing. See Figures 2c and 4 for location. Listric faults B1 and B2 on the upper slope deform late Miocene to Holocene sediments and offset the seafloor, with seaward facing scarps of ~25 m height. Fault B2 is characterized by growth strata. TWTT, two-way travel time. Vertical exaggeration ~ 2:1 at seafloor.

Research Program (NURP) in 1994. Side-scan sonar images revealed a fault and associated scarps with a N-S trend, traceable for 5 km. Submersible dives identified a series of terraces or scarps stepping down into the canyon, the uppermost of which offsets Pleistocene and Holocene sediments [*McNeill et al.*, 1995; *Piper et al.*, 1995]. Figure 8 shows a video frame taken during Delta submersible dive 3417 along Fault A1 (location in Figures 4 and 5) which reveals a fault scarp; the camera points to the northeast, and the scarp is ~ 0.5-1.0 m in height. Light gray Pleistocene clays and a thin cover of overlying olive-green Holocene hemipelagic sediment are exposed in the fault scarp, indicating fault movement during the Holocene. The scarp is relatively free from major bioturbation and hemipelagic sedimentation, suggesting fairly recent movement. Angular broken boulders are observed at the base of the scarp which also indicate recent breakage associated with fault movement or gravitational collapse at the head of the canyon. Side-scan sonar surveys of faults A1 and A2 provided evidence of active fluid venting in the form of precipitated calcium carbonate (high backscatter) which also suggests that these faults have been recently active [*Kulm and Suess*, 1990].

Where listric faulting occurs close to the shelf break and is associated with submarine canyon activity (e.g., Figure 4), the upper MBF contact or décollement rises to the west to become E-dipping and the MBF is commonly the source of diapiric intrusions. This reflects the mobility of the MBF unit and probably results from removal of the overlying sedimentary

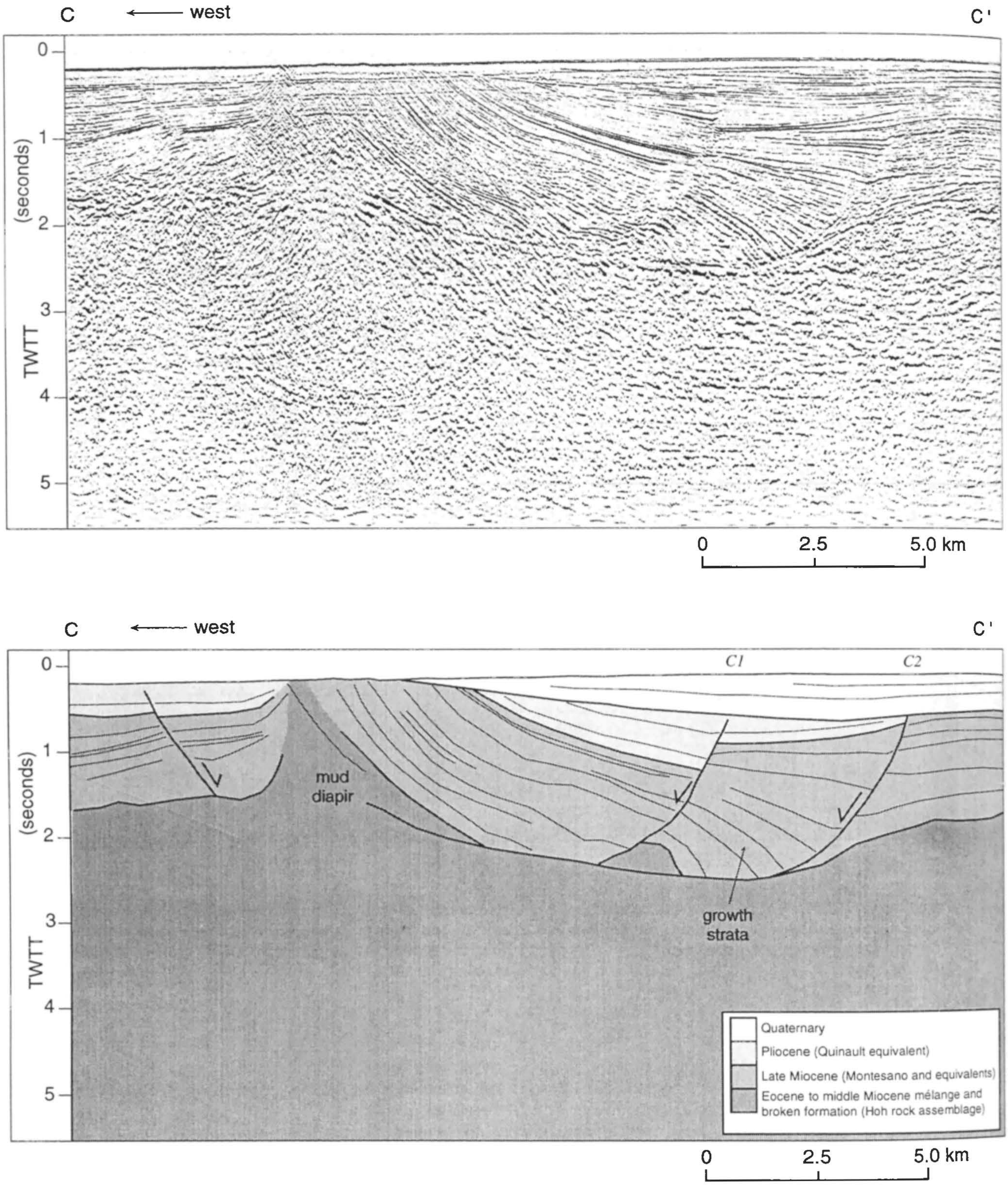

Figure 7. (Top) E-W migrated multichannel seismic reflection profile C-C' on the southern Washington midshelf off Willapa Bay with (bottom) interpretive line drawing. See Figure 2c for location. Listric faults C1 and C2 deform mid-Miocene (mélange and broken formation) to Pliocene sediments and are overlain by the undeformed Plio-Pleistocene unconformity. The growth strata are uplifted by a mud diapir rooted in the mélange to the west. Note also an east dipping normal fault to the west of the diapir. TWTT, two-way travel time. Vertical exaggeration ~ 2:1 at seafloor.

Figure 8. Video frame from the Delta submersible of fault scarp A1 (see Figures 4 and 5) at the head of Grays Canyon. Video camera points NE and two dots represent parallel laser beams placed 20 cm apart. The scarp is ~ 0.5-1 m in height. Scarp is relatively free from bioturbation and hemipelagic sediment, and angular boulders are observed at the base of the scarp, both suggesting recent activity.

load on the uppermost continental slope where erosion and slumping are common, particularly at the heads of submarine canyons. This phenomenon can be seen at the western end of seismic profile A-A' (Figure 5). In this same profile, east dipping normal faults with associated growth strata can be seen overlying the east dipping décollement to form full graben structures with west dipping faults, e.g., A1 and A2.

Discussion

Isolation of Shelf Tectonics

Normal faults in the Grays Canyon area (Figure 4), which indicate ~E-W extension, coexist with apparent compressional structures which suggest ~E-W shortening. Both sets of structures were apparently concurrently active throughout the Pliocene, and in some cases, during the Pleistocene and Holocene. Other workers [e.g., *Silver*, 1972; *Wagner et al.*, 1986] also suggest that this region of the Washington shelf is characterized by predominantly E-W shortening during the Neogene. However, recent coastal mapping [*McCrory*, 1994, 1996; *Thackray*, 1994] and our mapping of the inner continental shelf (C. Goldfinger and L.C. McNeill, manuscript in preparation, 1997) show evidence of active N-S shortening, suggesting that strain from oblique convergence is partitioned into arc-normal (E-W) and arc-parallel (N-S) components. This is supported by seismicity, structural data, and borehole breakouts onshore which also suggest N-S compression [e.g., *Spence*, 1989; *Zoback and Zoback*, 1990]. It is difficult to reconcile contemporaneous E-W extension and E-W shortening unless (1) the observed extension is a shallow and superficial effect, (2) predominantly nontectonic extension is occurring through some form of gravitational collapse, or (3) extension is nonsuperficial and the two tectonic regimes are isolated from one another. N-S compression and E-W extension may be dominant on much of the continental shelf, being mutually compatible stress regimes, and E-W compression is dominant on the lower slope, supporting hypothesis 3. In this scenario, N-S trending fold structures mapped on the shelf may be a result of gravitationally driven compression rather than interplate compression.

Association of Normal Faulting With Mélange and Broken Formation

The majority of listric normal faults sole out at depth to a subhorizontal décollement coincident with the uppermost strata of the middle Miocene MBF, indicating a strong link between extension and the MBF. The Hoh is chaotic, highly sheared, folded, and faulted in onshore exposures [*Palmer and Lingley*, 1989; *Orange*, 1990; *Orange et al.*, 1993] and contains abundant olistostromes, tectonic inclusions, and rip-up clasts [*Rau*, 1973; *Palmer and Lingley*, 1989]. Diapiric intrusions, both on the continental shelf [*Snavely and Wagner*, 1982] and in onshore outcrops [*Rau*, 1973; *Orange*, 1990], imply that the MBF is overpressured at depth [*Snavely*, 1987]. High mud weights required for drilling boreholes and increased mud pressure gradients in industry boreholes off northern Oregon, Washington, and southern Vancouver Island [*Snavely*, 1987; *Palmer and Lingley*, 1989] both point to elevated pore pressures within the MBF.

The distribution of major normal faults mapped to date on the Washington and northern Oregon continental shelf and upper slope (Figure 2c) coincides with the distribution of the underlying MBF unit, where it occurs immediately below late

Tertiary strata (Figure 1). The remainder of the northern and central Oregon continental shelf is underlain by the basaltic basement of the lower Eocene Siletz River Volcanics, part of the Coast Range basaltic basement or Siletzia terrane (Figure 1). The western boundary of the Siletz River Volcanics has been fairly confidently mapped from modeling magnetic and gravity anomalies, and seismic reflection profiles (Figure 1) [*Tréhu et al.*, 1994, 1995; *Fleming*, 1996]. The rigidity of the basalt contrasts with the sheared mélange and broken formation underlying the Washington and northernmost Oregon shelf and explains the absence of normal faulting [*McNeill et al.*, 1995]. The MBF may be underplated, in the form of sediment duplexing, beneath the Siletz River Volcanics. The Coast Range basaltic basement thins to the north and crops out onshore in Washington as the early to middle Eocene Crescent Formation, which includes the peripheral rocks of the Olympic Mountains [*Tabor and Cady*, 1978]. The Crescent Formation wraps around the Olympic core rocks and is found offshore as the Crescent and Metchosin Formations off the northwestern Olympic Peninsula (Figure 1). No listric normal faults have been identified overlying the inferred position of the northernmost Coast Range basaltic basement, but the seafloor morphology and Quaternary strata of this region are obscured by glacial outwash features from the Juan de Fuca lobe of the Cordilleran ice sheet. In southern coastal Oregon, the western boundary of the Siletz River Volcanics crosses the shoreline (Figure 1), and the basaltic basement is absent from the continental shelf. To date, no listric normal faults have been identified on the southern Oregon shelf or upper slope, although extremely large-scale slumping with prominent headwall scarps has been documented on the southern Oregon slope [*Goldfinger et al.*, 1995].

Cascadia Normal Faulting Mechanisms

The mélange and broken formation appears to control both the normal fault distribution and the timing of faulting, beginning in the late Miocene, following deposition, uplift, and erosion of the middle Miocene MBF. The MBF appears to decouple the overlying continental shelf sediments, characterized by extensional deformation, from subduction-controlled E-W to NE-SW compressional deformation evident on the lower continental slope. Two related mechanisms of decoupling are described below, involving, first, detachment of the basinal shelf sediments from the MBF, and secondly, mobilization and extension of the MBF.

The upper contact of the MBF, represented by the middle to late Miocene unconformity and downward transition in acoustic character from well-stratified to discontinuous reflectors, dips very gently west throughout much of the continental shelf (Figure 9), with measured slopes from the midshelf to the shelf break of approximately 0.1°-2.5°. These gentle seaward slopes represent the regional dip of this upper contact, ignoring local vertical variations due to faulting and folding. We hypothesize that such a shallow surface dip may be sufficient to allow unstable gravitational sliding on the upper MBF surface due to low basal friction and consequent detachment of the overlying sediments (Figures 9a and 9b). This mechanism can be used to explain extension along only the listric normal faults which sole out at depth into the upper MBF contact. The reduced strength and effective shear stress along a fault plane or detachment associated with high pore

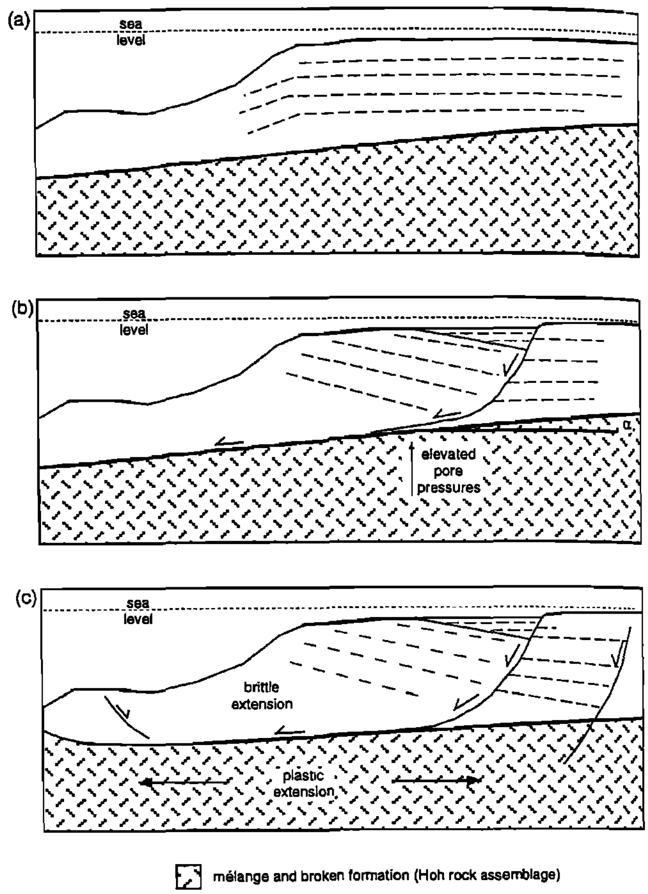

Figure 9. Development and mechanisms of listric faulting on the Cascadia outer shelf. (a) Prior to extension: mélange and broken formation (MBF) deposited at bathyal depths, uplifted, and eroded, and overlying late Miocene sediments deposited. The upper MBF contact dips gently seaward. (b) Extensional failure occurring through gravitational collapse along a detachment separating the MBF and overlying sediments. Elevated pore pressures within the MBF increase the chance of movement on the low-dipping failure plane. Dip of the mélange surface, $\alpha \approx 0.1°\text{-}2.5°$. (c) Mobilization and extension of the MBF results in brittle extension of the overlying sediments. East dipping normal faults also form.

fluid pressures has been documented by *Hubbert and Rubey* [1959] in the theory of low-angle overthrust faulting or gravitational sliding and by *Davis et al.* [1983] in the Coulomb theory of the critical tapered wedge. Seaward or downslope dipping listric normal faults also support gravitational sliding as a mechanism of extension. The upper MBF contact (middle to late Miocene unconformity) thus may act as a detachment [*Piper*, 1994], separating the mobile MBF and the more rigid post-MBF sediments, along which the late Miocene to Quaternary section moves downslope (Figure 9b). The listric faults on the Cascadia margin may therefore be similar to growth faults on the Texas coast, where faults flatten at depth into low-density, high fluid pressure shale masses [*Bruce*, 1973]. Normal faulting at the base of the Guatemalan slope is also thought to be a result of decoupling through elevated pore fluid pressures, as encountered during Leg 84 of the Deep Sea Drilling Project [*Aubouin et al.*, 1982], although this margin is characterized by much steeper terrain.

The subhorizontal upper contact of the MBF on the continental shelf and upper slope suggests mobilization and redistribution of this unit, aided by gravitationally driven downslope movement. The MBF may therefore be undergoing mobilization and extension to the west, where it is apparently unconstrained, with accompanying rigid or brittle extension of the overlying younger deposits (Figures 9a and 9c). The upper contact may still behave as a detachment, as hypothesized above, but in this case, both the mobile MBF and the overlying brittle section undergo extension, with reduced relative displacement between these two units. There may be an additional detachment at depth within the MBF, below which no extension occurs, resulting from increases in strength or decreases in pore fluid pressure. Mobilization and extension of the MBF comprise a preferred explanation for listric faults which do not flatten into a sub-horizontal décollement, but penetrate and offset the MBF unit. Diapiric intrusions throughout the shelf and evidence of upward movement of the MBF at the shelf edge (Figures 5 and 9c), where the overlying sedimentary load is reduced, point to significant mobilization. Extension of both the mobile MBF and overlying brittle sediments explains the presence of east dipping and apparently upslope dipping normal faults on the shelf and upper slope (e.g., western end of Figure 5). These faults are less easily explained by downslope movement on a seaward-dipping detachment. Extension and thinning of the Hoh beneath the shelf might be expected to result in net subsidence, which contradicts paleobathymetric evidence of net uplift during the period of extension [*Rau*, 1970; *Bergen and Bird*, 1972]. This apparent contradiction can, however, be explained by the counteraction of other factors influencing the uplift history of the shelf, including sedimentation rates, sediment underplating, and the variation of subducting slab dip.

Extension and thinning of the MBF are supported by the increased width (Figure 1) and low taper angle of the Washington and northern Oregon margins relative to those of the central and southern Oregon margins. Mapped fold trends (Figure 2a) appear to wrap around a feature on the upper slope of the central Washington margin which is coincident with a convex-seaward "protrusion" or "bulge" in the shelf edge and is also indicated by shaded relief bathymetry [*Haugerud*, 1996]. We hypothesize that this protrusion and anomalous fold trends represent the expression of downslope movement and extension of the MBF (movement indicated by arrows in Figure 2a). The absence of similar seafloor morphology and structure to the north and south cannot be presently explained but may be the result of reduced tilting of the MBF or a constraining structure reducing seaward extension. It is interesting to note that the many of the normal faults mapped coincide with this anomaly in fold trends opposite Grays Harbor (Figures 2a and 2c).

The presence of both normal faults (listric and potentially nonlistric) that cut the MBF and those that deform only overlying sediments implies that both motion on the detachment and westward flow of the MBF are occurring. Both mechanisms have been proposed as models for extension in earlier work on metamorphic core complexes of the Basin and Range Province [*Wernicke*, 1981].

Alternative Faulting Mechanisms

Westward or seaward extension resulting from both downslope movement on the upper MBF detachment and from extension within the MBF may be accentuated by uplift and westward tilting of the continental shelf and upper slope. Uplift of the shelf would increase the slope beyond a critical angle resulting in gravitational collapse. Such mechanisms are not thought necessary for extension to occur on the Washington and northern Oregon margin, but may increase the rate of movement on the MBF detachment and downslope movement of the MBF, or prolong the period of extension. Evidence of vertical tectonics on the shelf and upper slope (Figure 3) and the uplifted Olympic Mountains onshore [*Brandon and Calderwood*, 1990] indicate broadly contemporaneous uplift through the Miocene and Pliocene, coincident with listric normal faulting. Uplift of the shelf could be caused by underplating of subducted sediments beneath the shelf, resulting in westward tilt.

An alternative mechanism is the differential compaction or loading of the overpressured mobile MBF resulting in diapiric intrusions and growth faulting, as frequently observed on passive margins underlain by mobile sediments such as shale or salt [e.g., *Morley and Guerin*, 1996]. Diapirism is locally found in direct association with listric normal faulting on the Cascadia margin. Figure 7 shows two listric faults, C1 and C2, active during the late Miocene and Pliocene, associated with a diapiric intrusion rooted in the MBF below the listric faults. A requirement of differential loading is variation in the overburden mass, which is produced where basins or normal-fault-bounded depocenters exist. Therefore differential loading may only be responsible for initiation of faulting at the edges of preexisting basins or perpetuating movement on pre-existing faults. Differential loading is subsequently a self-sustaining process, with increased basinal deposition leading to further compaction and associated growth faulting and diapirism. This mechanism is a result of vertical movement of the mobile unit in contrast to that of gravity-induced downslope movement where horizontal motions are involved. Differential loading may be locally significant but secondary to horizontal mobilization of the MBF on a regional scale.

Two of the mapped listric faults are located at the heads of Grays and Quinault submarine canyons (Figures 2c and 4), suggesting some association between faulting and canyon formation [*McNeill et al.*, 1995; *Piper et al.*, 1995]. The longevity of normal faulting (late Miocene to present) relative to the short lifespan of submarine canyons (present canyons were probably formed during Pleistocene lowstands) suggests that canyon formation may have been locally controlled by faulting, due to the preexisting plane of weakness along the fault, rather than canyons influencing fault location.

Extension Versus Compressional Deformation

Current extension of the continental shelf and upper slope is contemporaneous with accretion and thrust faulting on the lower slope of the accretionary wedge (Figure 2a). In addition, extensional faulting appears to be contemporaneous with mapped fold structures of C. Goldfinger and L.C. McNeill (manuscript in preparation, 1997) and other workers on the continental shelf (Figures 2a, 2c, and 4). In the light of the evidence for mobile extension, we have reexamined our earlier mapping and conclude that many of the folds in the vicinity of the normal faults are rollover folds, drape structures, and folds driven by downslope spreading of the MBF. These structures could be misinterpreted as purely convergence-related structures without the high quality data set used for this study.

E-W contractile strain is apparently low on the shelf and upper slope. We hypothesize that the extensional tectonic regime of this region is isolated by the mobile MBF from the convergence-related E-W to NE-SW compression on the lower slope. Figure 2a delineates zones of compression and extension determined from existing data. Extension extends seaward to the upper slope, and the prominent bulge may mark the seaward edge of the MBF, and therefore extension, on the central Washington margin. The midslope area, lying between these two regions of known compression and extension, may act as a transition zone or, more likely, a distinct change from extension to compression is located in this area. The seaward extent of the MBF is uncertain, and the resolution of available data may prevent the identification of extensional faults on much of the slope. The thickness and strength of the older MBF are unknown, and therefore the depth to which extension extends is unclear: a deeper compressional regime may underlie the extending MBF. The presence of E-W trending folds on the inner continental shelf suggests that N-S compression and E-W extension are operating simultaneously. An extreme case of decoupling extending to the plate interface (10-15 km beneath the shelf) would have significant implications for the extent of coupling on the subduction zone and hence position and width of the interplate locked zone. The extent and significance of decoupling induced by the MBF are the subject of further study and cannot be fully addressed in this paper.

Global Comparisons

Extension on the Cascadia margin differs significantly from the transient nature of extension observed in many other convergent margins. A commonly cited mechanism for extension in such margins is subduction erosion at the base or the front of the wedge. Forearc oversteepening, extensional faulting, and slope failure have been attributed to subduction erosion as a result of subduction of seamounts (Japan trench [*von Huene and Lallemand*, 1990]), a ridge (Peru trench [*von Huene and Lallemand*, 1990]), or horst and graben structures (Middle America Trench off Guatemala [*Aubouin et al.*, 1982] and Japan trench [*von Huene and Lallemand*, 1990]). The subduction of elevated basement features produces a local short-term extension or with a sweeping effect along the margin if a linear structure is subducted at an oblique angle, such as the subduction of the Nazca ridge beneath the Peru margin [*von Huene and Lallemand*, 1990]. However, extensional faulting in offshore Washington and northern Oregon is too regional and long-term (late Miocene to present) to be associated with the subduction of a discrete linear basement feature. In addition, subduction erosion would be accompanied by subsidence, which is not supported by paleobathymetric evidence, indicating net uplift through the Miocene and Pliocene [*Rau*, 1970; *Bergen and Bird*, 1972].

The dominance of extensional deformation on the shelf and upper slope in contrast to the expected compressional deformation of a convergent margin is common to the margins of Japan, Peru [*von Huene and Lallemand*, 1990], Costa Rica [*McIntosh et al.*, 1993], and the margin of Shumagin, Alaska [*Bruns et al.*, 1987], in addition to northern Cascadia. Extension and basinal deposition on the landward margin is concurrent with, and isolated from, accretion on the lower slope, as observed on the Cascadia margin. Basins on these margins, e.g., Lima Basin in Peru, Joban Basin in Japan, and Shumagin, Sanak, and Unimak Basins in Alaska, overlie a regional unconformity, suggesting rapid regional subsidence and crustal thinning. Mechanisms of extension may differ between these examples but all result in isolation of extension and compression.

Conclusions

Listric normal faulting appears to be the result of (1) downslope movement along a low-angle décollement between the uppermost middle Miocene MBF and the overlying basinal sediments and (2) mobilization and extension of the MBF and consequent brittle extension of the overlying sediments. Miocene and Pliocene uplift of the continental shelf may have resulted in oversteepening of the shelf and further gravitational collapse but was probably not a requirement for extension. The subsurface distribution of the MBF restricts extension to the Washington and northern Oregon shelf and upper slope.

Contemporaneous compressional tectonics of the lower slope and extensional tectonics of the shelf and upper slope are apparently isolated from each other, with the latter region being decoupled from the E-W compressional forces of convergence by the underlying mobile material. Such segregation of extensional and compressional regimes on convergent margins is not unique to Cascadia, with similar observations on the Peru, Japan, Costa Rica, and Alaskan margins. Many N-S trending fold structures previously interpreted as tectonic expressions of convergence-related compression, including rollover folds, drape folds, and hanging wall synclines, can be attributed to listric faulting, with E-W extension being the dominant tectonic style. We conclude that E-W contractile strain is low on the Washington and northern Oregon shelf and that a transition from extension to compression occurs in the mid slope region, likely coincident with the seaward edge of the MBF (Figure 2a). The presence of long-term major extensional faults, which displace sediments to depths of 2-3 km or greater throughout much of the northern Cascadia continental shelf and upper slope, is of importance to the current stability of the margin.

Acknowledgments. We acknowledge the Minerals Management Service Pacific OCS Region at Camarillo, California for supplying data necessary for this study and Scott Drewry of MMS for use of his unpublished work. We thank Steve Dickenson and Robert Lillie for helpful discussion and J.H. McBride, R. von Huene, and G.K. Westbrook for thorough and helpful reviews. We also thank the crew of the *Cavalier*, Delta submersible pilots Dave Slater and Chris Ijames, members of the 1994 scientific party (Paul Crenna, Gary Huftile, Cheryl Hummon, Alan Niem, Brad Thurber, and Hiro Tsutsumi), and Kevin Redman, David Wilson, Tim McGiness, Chris Center, and Kirk O'Donnell of Williamson and Associates, Seattle, Washington, for side-scan sonar operations. This study was supported by NOAA Undersea Research Program at the West Coast National Undersea Research Center at the University of Alaska grants UAF-92-0061 and UAF-93-0035, National Science Foundation grants OCE-8812731 and OCE-9216880, and U.S. Geological Survey National Earthquake Hazards Reduction Program awards 14-08-0001-G1800, 1434-93-G-2319, 1434-93-G-2489, and 1434-95-G-2635.

References

Aubouin, J., et al., Leg 84 of the Deep Sea Drilling Project: Subduction without accretion: Middle America Trench off Guatemala, *Nature*, *297*, 458-460, 1982.

Bergen, F.W., and K.J. Bird, The biostratigraphy of the Ocean City area, Washington, in *The Pacific Coast Miocene Biostratigraphic Symposium, Proceedings*, pp. 173-191, Econ. Paleontol. and Mineral. Pac. Sect., 1972.

Brandon, M.T., and A.R. Calderwood, High-pressure metamorphism and uplift of the Olympic subduction complex, *Geology*, *18*, 1252-1255, 1990.

Bruce, C.H., Pressured shale and related sediment deformation: Mechanism for development of regional contemporaneous faults, *AAPG Bull.*, *57*, 878-886, 1973.

Bruns, T.R., R. von Huene, R.C. Culotta, S.D. Lewis, and J.W. Ladd, Geology and petroleum potential of the Shumagin margin, Alaska, in *Geology and Resource Potential of the Continental Margin of Western North America and Adjacent Ocean Basins-Beaufort Sea to Baja California*, edited by D. W. Scholl, A. Grantz, and J.G. Vedder, pp. 157-189, Circum-Pac. Counc. for Energy and Miner. Resour., Houston, Tex., 1987.

Busch, D.A., Influence of growth faulting on sedimentation and prospect evaluation, *AAPG Bull.*, *59*, 217-230, 1975.

Carson, B., J. Yuan, P.B. Myers Jr., and W.D. Barnard, Initial deep-sea sediment deformation at the base of the Washington continental slope: A response to subduction, *Geology*, *2*, 561-564, 1974.

Cranswick, D.J., and K.A. Piper, Geologic framework of the Washington-Oregon continental shelf—Preliminary findings, in *Proceedings of the 1991 Exclusive Economic Zone Symposium on Mapping and Research: Working Together in the Pacific EEZ*, *U.S. Geol. Surv. Circ.*, *1092*, 146-151, 1992.

Dahlen, F.A., Noncohesive critical Coulomb wedges: An exact solution, *J. Geophys. Res.*, *89*, 10,125-10,133, 1984.

Davis, D., J. Suppe, and F.A. Dahlen, Mechanics of fold-and-thrust belts and accretionary wedges, *J. Geophys. Res.*, *88*, 1153-1172, 1983.

DeMets, C., R.G. Gordon, D.F. Argus, and S. Stein, Current plate motions, *Geophys. J. Int.*, *101*, 425-478, 1990.

Fleming, S.W., Bulldozer blades and colliding submarine mountain chains: Constraints on central Oregon convergent margin tectonics from magnetics and gravity, M.S. thesis, 84 pp., Oreg. State Univ., Corvallis, 1996.

Goldfinger, C., L.D. Kulm, and R.S. Yeats, Neotectonic map of the Oregon continental margin and adjacent abyssal plain, scale 1:500,000, *Open File Rep. O-92-4*, Oreg. Dep. of Geol. and Mineral Ind., Portland, 1992.

Goldfinger, C., L.D. Kulm, and L.C. McNeill, Super-scale slumping of the southern Oregon Cascadia margin: Tsunamis, tectonic erosion, and extension of the forearc, *Eos Trans. AGU*, *76*(46), Fall Meet. Suppl., F361, 1995.

Haugerud, R.A., Digital topographic-bathymetric map of Cascadia (39°N-53°N, 116°W-133°W), *Geol. Soc. Am. Abstr. Programs*, *28*(5), 73, 1996.

Hubbert, M.K., and W.W. Rubey, Role of fluid pressure in mechanics of overthrust faulting, 1, Mechanics of fluid-filled porous solids and its application to overthrust faulting, *Geol. Soc. Am. Bull.*, *70*, 115-166, 1959.

Karig, D.E., H. Kagami, and DSDP Leg 87 Scientific Party, Varied responses to subduction in Nankai Trough and Japan forearc, *Nature*, *304*, 148-151, 1983.

Kleinpell, R.M., *Miocene Stratigraphy of California*, 450 pp., T. Murby, London, 1938.

Kulm, L.D., and G.A. Fowler, Oregon continental margin structure and stratigraphy: A test of the imbricate thrust model, in *The Geology of Continental Margins*, edited by C.A. Burk and C.L. Drake, pp. 261-284, Springer-Verlag, New York, 1974.

Kulm, L.D., and E. Suess, Relation of carbonate deposits and fluid venting: Oregon accretionary prism, *J. Geophys. Res.*, *95*, 8899-8915, 1990.

Kulm, L.D., R.A. Prince, and P.D. Snavely Jr., Site survey of the northern Oregon continental margin and Astoria Fan, *Initial Rep. Deep Sea Drill. Proj.*, *18*, 979-987, 1973.

Li, C., Forearc structures and tectonics in the southern Peru-northern Chile continental margin, *Mar. Geophys. Res.*, *17*, 97-113, 1995.

MacKay, M.E., G.F. Moore, G.R. Cochrane, J.C. Moore, and L.D. Kulm, Landward vergence and oblique structural trends in the Oregon margin accretionary prism: Implications and effect on fluid flow, *Earth Planet. Sci. Lett.*, *109*, 477-491, 1992.

Mallory, V.S., *Lower Tertiary Biostratigraphy of the California Coast Ranges*, 416 pp., Am. Assoc. of Pet. Geol., Tulsa, Okla., 1959.

McCaffrey, R., and C. Goldfinger, Forearc deformation and great subduction earthquakes: Implications for Cascadia earthquake potential, *Science*, *267*, 856-859, 1995.

McClain, K.J., A geophysical study of accretionary processes on the Washington continental margin, Ph.D. thesis, 141 pp., Univ. of Wash., Seattle, 1981.

McCrory, P.A., Quaternary crustal shortening along the central Cascadia subduction margin, Washington, *Geol. Soc. Am. Abstr. Programs*, *26*(7), A-523, 1994.

McCrory, P.A., Tectonic model explaining divergent contraction directions along the Cascadia subduction margin, Washington, *Geology*, *24*, 929-932, 1996.

McIntosh, K., E. Silver, and T. Shipley, Evidence and mechanisms for forearc extension at the accretionary Costa Rica convergent margin, *Tectonics*, *12*, 1380-1392, 1993.

McNeill, L.C., K.A. Piper, C. Goldfinger, and L.D. Kulm, Detachment faulting on the Cascadia continental shelf: Active extension in a compressional regime?, *Eos Trans. AGU*, *76*(46), Fall Meet. Suppl., F534, 1995.

Morley, C.K., and G. Guerin, Comparison of gravity-driven deformation styles and behavior associated with mobile shales and salt, *Tectonics*, *15*, 1154-1170, 1996.

Natland, M.L., Pleistocene and Pliocene stratigraphy of southern California, Ph.D. thesis, 165 pp., 20 plates, Univ. of Calif., Los Angeles, 1952.

Orange, D.L., Criteria helpful in recognizing shear-zone and diapiric mélanges: Examples from the Hoh accretionary complex, Olympic Peninsula, Washington, *Geol. Soc. Am. Bull.*, *102*, 935-951, 1990.

Orange, D.L., D.S. Geddes, and J.C. Moore, Structural and fluid evolution of a young accretionary complex: The Hoh rock assemblage of the western Olympic Peninsula, Washington, *Geol. Soc. Am. Bull.*, *105*, 1053-1075, 1993.

Palmer, S.P., and W.S. Lingley, An assessment of the oil and gas potential of the Washington outer continental shelf, *Rep. WSG 89-2*, 88 pp., Wash. Sea Grant Program, Seattle, Wash., 1989.

Piper, K.A., Extensional tectonics in a convergent margin—Pacific Northwest offshore, Washington and Oregon, *AAPG Bull.*, *78*, 673, 1994.

Piper, K.A., L.C. McNeill, and C. Goldfinger, Active growth faulting on the Washington continental margin, *AAPG Bull.*, *79*, 596, 1995.

Rau, W.W., Foraminifera, stratigraphy, and paleoecology of the Quinault Formation, Point Grenville-Raft River coastal area, Washington, *Wash. Div. Mines Geol. Bull.*, *62*, 41 pp., 1970.

Rau, W.W., Geology of the Washington coast between Point Grenville and the Hoh River, *Wash. Div. Geol. Earth Resour. Bull.*, *66*, 58 pp., 1973.

Rau, W.W., Geologic map of the Destruction Island and Taholah quadrangles, Washington, scale 1:63,360, *Geol. Map GM-13*, Wash. Div. of Geol. and Earth Resour., Olympia, Wash., 1975.

Rau, W.W., Geologic map in the vicinity of the lower Bogachiel and Hoh River valleys, and the Washington coast, scale 1:62,500, *Geol. Map GM-24*, Wash. Div. of Geol. and Earth Resour., Olympia, Wash., 1979.

Rau, W.W., Pacific Northwest Tertiary benthic foraminiferal biostratigraphic framework—An overview, *Spec. Pap. Geol. Soc. Am.*, *184*, 67-84, 1981.

Shor, G.G., P. Dehlinger, H.K. Kirk, and W.S. French, Seismic refraction studies off Oregon and northern California, *J. Geophys. Res.*, *73*, 2175-2194, 1968.

Silver, E.A., Pleistocene tectonic accretion of the continental slope off Washington, *Mar. Geol.*, *13*, 239-249, 1972.

Snavely, P.D., Jr., Tertiary geologic framework, neotectonics, and petroleum potential of the Oregon-Washington continental margin, in *Geology and Resource Potential of the Continental Margin of Western North America and Adjacent Ocean Basins-Beaufort Sea to Baja California*, edited by D. W. Scholl, A. Grantz, and J.G. Vedder, pp. 305-335, Circum-Pac. Counc. for Energy and Miner. Resour., Houston, Tex., 1987.

Snavely, P.D., Jr., and K.A. Kvenvolden, Preliminary evaluation of the petroleum potential of the Tertiary accretionary terrane, west side of the Olympic Peninsula, 1, Geology and hydrocarbon potential, *U.S. Geol. Surv. Bull.*, *1892*, 1-18, 1989.

Snavely, P.D., Jr., and P.H. McClellan, Preliminary geologic interpretation of USGS S.P. Lee seismic reflection profile WO 76-7 on the continental shelf and upper slope, northwestern Oregon, *U.S. Geol. Surv. Open File Rep.*, *87-612*, 12 pp., 1987.

Snavely, P.D., Jr., and H.C. Wagner, Geologic cross section across the continental margin of southwestern Washington, *U.S. Geol. Surv. Open File Rep.*, *82-459*, 10 pp., 1982.

Snavely, P.D., Jr., and R.E. Wells, Cenozoic evolution of the continental margin of Oregon and Washington, *U.S. Geol. Surv. Open File Rep.*, *91-441B*, 34 pp., 1991.

Spence, W., Stress origins and earthquake potential in Cascadia, *J. Geophys. Res.*, *94*, 3076-3088, 1989.

Tabor, R.W., and W.M. Cady, The structure of the Olympic Mountains, Washington—Analysis of a subduction zone, *U.S. Geol. Surv. Prof. Pap.*, *1033*, 38 pp., 1978.

Thackray, G. D., Deformation of middle and late Pleistocene strata on the Olympic coast of Washington, *Geol. Soc. Am. Abstr. Programs*, *26*(7), A-523, 1994.

Tréhu, A.M., I. Asudeh, T.M. Brocher, J.H. Luetgert, W.D. Mooney, J.L. Nabelek, and Y. Nakamura, Crustal architecture of the Cascadia forearc, *Science*, *265*, 237-243, 1994.

Tréhu, A., G. Lin, E. Maxwell, and C. Goldfinger, A seismic reflection profile across the Cascadia subduction zone offshore central Oregon: New constraints on methane distribution and crustal structure, *J. Geophys. Res.*, *100*, 15,101-15,116, 1995.

von Huene, R., and S. Lallemand, Tectonic erosion along the Japan and Peru convergent margins, *Geol. Soc. Am. Bull.*, *102*, 704-720, 1990.

von Huene, R., and D.W. Scholl, Observations at convergent margins concerning sediment subduction, subduction erosion, and the growth of continental crust, *Rev. Geophys.*, *29*, 279-316, 1991.

von Huene, R., J. Bourgois, J. Miller, and G. Pautot, Massive collapse along the front of the Andean convergent margin off Peru, *J. Geophys. Res.*, *94*, 1703-1714, 1989.

Wagner, H.C., L.D. Batatian, T.M. Lambert, and J.H. Tomson, Preliminary Geologic framework studies showing bathymetry, locations of geophysical tracklines and exploratory wells, seafloor geology and deeper geologic structures, magnetic contours, and inferred thickness of Tertiary rocks on the continental shelf and upper continental slope of southwest Washington between latitudes 46°N and 48° 30'N and from the Washington coast to 125° 30'W, *Open File Rep. 86-1*, 10 pp., Wash. Div. of Geol. and Earth Resour., Olympia, Wash., 1986.

Wernicke, B., Low-angle normal faults in the Basin and Range Province: Nappe tectonics in an extending orogen, *Nature*, *291*, 645-647, 1981.

Westbrook, G.K., et al., *Proceedings of the Ocean Drilling Program, Initial Reports*, *146* , 92 pp., Ocean Drill. Program, College Station, Tex., 1994.

Wilson, D.S., Confidence intervals for motion and deformation of the Juan de Fuca plate, *J. Geophys. Res.*, *98*, 16,053-16,071, 1993.

Zoback, M.L., and M.D. Zoback, Tectonic stress field of the continental United States, in *Geophysical framework of the Continental United States, Mem. Geol. Soc. Am.*, edited by L. Pakiser and W. Mooney, *172*, 523-540, 1990.

C. Goldfinger and L.D. Kulm, College of Oceanic and Atmospheric Sciences, Oregon State University, Corvallis, Oregon 97331. (e-mail: gold@oce.orst.edu; kulm@oce.orst.edu)

L.C. McNeill and R.S. Yeats, Department of Geosciences, Oregon State University, Corvallis, Oregon 97331. (e-mail: lmcneill@oce.orst.edu; yeatsr@bcc.orst.edu)

K.A. Piper, Minerals Management Service, Camarillo, California 93010. (e-mail: kenneth_piper@smtp.mms.gov)

(Received July 29, 1996; revised February 27, 1997; accepted March 7, 1997.)